Enhanced light emission efficiency and current stability by morphology control and thermal annealing of organic light emitting diode devices

2006 J. Phys.: Condens. Matter 18 S2139

(http://iopscience.iop.org/0953-8984/18/33/S29)

INSTITUTE OF PHYSICS PUBLISHING JOURNAL OF PHYSICS: CONDENSED MATTER

J. Phys.: Condens. Matter **18** (2006) S2139–S2147 doi:10.1088/0953-8984/18/33/S29

Enhanced light emission efficiency and current stability by morphology control and thermal annealing of organic light emitting diode devices

S Caria[1,3], E Da Como[1], M Murgia[1], R Zamboni[1], P Melpignano[2] and V Biondo[2]

[1] Consiglio Nazionale delle Ricerche (CNR), Istituto per lo Studio dei Materiali Nanostrutturati (ISMN), Via P Gobetti 101, 40129 Bologna, Italy
[2] Centro Ricerche Plast-Optica (CRP), via Jacopo Linussio 1, 33020 Amaro (UD), Italy

E-mail: scaria@bo.ismn.cnr.it

Received 8 February 2006, in final form 13 June 2006
Published 4 August 2006
Online at stacks.iop.org/JPhysCM/18/S2139

Abstract

The electro-optical behaviour of organic light emitting diode devices (OLEDs) is greatly influenced by the morphology of the films. A major parameter is due to the important role that the morphology of the active organic thin films plays in the phenomena that lead to light emission. For vacuum-grown OLEDs, the morphology of the specific thin films can be varied by modification of the deposition conditions. We have assessed the method (ultrahigh-vacuum organic molecular beam deposition) and conditions (variation of the deposition rate) for electro-emission (EL) optimization in a standard α-NPB (N,N'-bis-(1-naphthyl)-N,N'diphenyl-1,1′biphenyl-4-4′diamine)/Alq3 (tris-(8-hydroxyquinoline) aluminium) vacuum-grown OLED device. The best EL performances have been obtained for OLEDs made in ultrahigh vacuum with the Alq3 layer deposited with a differential deposition rate ranging from $1.0 \rightarrow 0.3$ Å s^{-1}. The results are consistent with a model of different Alq3 morphologies, allowing efficient charge injection at the metal/organic interface, and of the minimization of grain boundaries at the electron–hole recombination interface, allowing efficient radiative excitonic decay. At the same time, with the objective of controlling and stabilizing the morphology changes and stabilizing the charge transport over a long OLED operating time, we have studied the effect of thermal annealing processing in the standard current behaviour of OLEDs. The large current fluctuations typically observed for standard vacuum-grown OLEDs have been smeared out and kept constant over a long operating time by the given thermal annealing conditions. The results are interpreted in terms of the stabilization of intrinsic polymorphism of the organic film's

[3] Author to whom any correspondence should be addressed.

structure induced by thermal energy and leading the morphology to a lowest-energetic configuration.

(Some figures in this article are in colour only in the electronic version)

1. Introduction

Significant progress in the fabrication of efficient organic light emitting diodes (OLED) has been made in the last few years, allowing the exploitation of glass-based OLED displays in the electronic market as fundamental components in mobile phones, flat panel displays [1, 2], mp3 players and other electronic goods. Moreover, OLEDs may have an even higher commercial impact if fully exploited as innovative solid-state light sources (which are cost effective and energy saving) [3], flexible displays and solid-state electrically pumped lasers. In this perspective, there has been a recent report [4] of a current density of up to 1000 A cm^{-2} in a conventional OLED, namely α-NPB (N,N'-bis-(1-naphthyl)-N,N'diphenyl-1,1′biphenyl-4-4′diamine)/Alq3 (tris-(8-hydroxyquinoline) aluminium) grown on rigid substrates (glass and silicon). This impressive result opens the way to the possibility of electrically pumped organic laser diodes.

However, despite these unquestionable successes, there are still unresolved fundamental problems (such as the charge transport mechanism in organic molecular solids) together with practical hurdles concerning OLED device applications. Among them, we can underline the light generation and extraction efficiency, the photo-chemical and electro-chemical degradation processes [5] and the device stability and performances over a given operating time. In particular, for real devices it is crucial to have a reliable current stability over a long operating time.

The behaviour of OLEDs is greatly influenced by the morphology of organic thin layers [6]. This is due to the important role that the morphology of the active organic thin films plays in the phenomena that lead to light emission. Schematically, they can be summarized in the following points: (1) charge injection, (2) charge transport, (3) the combination of the charges with exciton formation, and (4) the relaxation of an exciton to the ground state via radiative decay. A full check of the four points mentioned above allows the optimal exploitation of the potential of OLED-based devices. In this context, we have started a systematic experimental study aimed at optimizing stable light emission efficiency and current stability over long operating times of a standard OLED structure.

It is worth noting how organic thin films are generally polycrystalline. Moreover, it is well recognized how organic systems show polymorphism properties in the solid state. Usually, in a standard vacuum-grown OLED, small grain sizes that are fully interconnected are required at the organic–metal interface. This is a requirement for a reproducible, large number of charge injection points and, eventually, the best charge transport performance. This is particularly significant at the cathode interface [7] since, in standard OLEDs, the electron current is of the order of a magnitude lower than the current with holes. At the same time, at the interface where hole and electron recombination occurs, it is desirable to have organic grains that are substantially larger than the exciton diffusion length (typically of the order of 100–300 Å [8, 9]). In this region, in fact, the formation of excitons takes place, and larger organic grains mean a lower number of grain boundaries on which excitons could decay through a non-radiative path during their migration and consequently affect the radiative emission efficiency of the OLED device. Our strategy was aimed at controlling the size of the organic in the organic

layers by manipulating the thin-film deposition conditions, namely the deposition rate. It has been demonstrated [10, 11] that the thermal evaporation rate of organics affects the organic morphology of the films through the grain size of the layers and then the efficiency of the devices. In particular, we have attempted to obtain both situations described above in the Alq_3 layer.

In addition, standard OLEDs show a current behaviour that is characterized by large fluctuations during its operation time. This effect compromises the light emission as well. In this regard, we have made a systematic study of the I–V characteristics of a standard Alq_3-NPB OLED device towards the annealing temperature with the objective of controlling and stabilizing the morphology changes and stabilizing the charge transport over a long operating time.

2. Experimental details

Alq_3 (tris-(8-hydroxyquinoline) aluminium) and α-NPB (N,N'-bis-(1-naphthyl)-N,N'diphenyl-1, 1′biphenyl-4-4′diamine) materials, of 99%+ purity, were purchased from Aldrich and processed without any further purification. Organic thin films and metal contacts have been grown by an ultrahigh-vacuum (UHV)—organic molecular beam deposition (OMBD) [12] system, with a base pressure of 10^{-10} mbar. The OMBD system allows the fabrication of the designed OLED device *in situ*, i.e. without breaking the UHV conditions. Thin films made of a 55 nm thickness of α-NPB and a 65 nm thickness of Alq_3 were thermally sublimed from an effusion Knudsen cell and sequentially deposited onto a Barix™/Al or glass/ITO (indium tin oxide) substrate. Depending on the experiment, different deposition rates were selected. The electro-emission (EL) properties and electrical characteristics of the investigated OLEDs were examined in OMBD by transferring the OLED device into a characterization chamber (with a base pressure of 10^{-11} mbar) equipped with electrical contacts. The EL intensity emitted from the OLED has been measured by optical coupling through a quartz window and collected by a photomultiplier and/or an optical multichannel analyser. Simultaneously to the EL detection, the current voltage (I–V) characteristics of the investigated OLEDs were measured using a computer-controlled Keithley SMU-236 apparatus. All the substrates used were ultrasonically cleaned with suitable solvents and then ultaviolet (UV)-ozone treated for 5 min before being loaded into the deposition chamber. Confocal images were collected with a Nikon 2000 E laser scanning confocal microscope (LSCM). Details of the experimental set-up are reported in [13]. Schematically, LSCM images are obtained by scanning the exciting laser beam (Ar+ 488 nm) across the sample. The photoluminescence (PL) image is reconstructed point by point, with a lateral spatial resolution of 300 nm and a volume resolution of 400 nm, by recording the PL signal using a photomultiplier. In LSCM images, the brighter regions correspond to the highest PL emission intensity, while the darker regions have low emission intensity. With this technique, it is possible to investigate the characteristics of the morphology of organic thin films. Thermal treatments of the OLED devices and/or of the selected organic moieties used in the thin film for OLED fabrication were performed in UHV *in situ* in the OMBD system by a resistive heater placed in the sample holder from room temperature up to 130 °C.

3. Results and discussion

3.1. Effect of morphology of organic films on efficiency of OLEDs

Relations between deposition rates, OLED behaviour and associated morphologies were studied on a standard vertical architecture, namely a 65 nm thick Alq_3 (tris-(8-

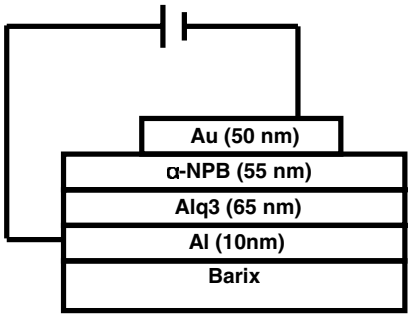

Figure 1. Schematic of the architecture of devices built on a flexible substrate: Barix/Al(10 nm)/Alq_3(65 nm)/α-NPB(55 nm)/Au(100 nm).

hydroxyquinoline) aluminium) thin film as an electron transport layer and emitter layer and a 55 nm thick α-NPB (N,N'-bis-(1-naphthyl)-N,N'diphenyl-1,1′biphenyl-4-4′diamine) thin film as a hole transport layer. Flexible Barix^{TM} foils (supplied by Vitex System) have been used as substrates. This substrate represents the state of the art in flexible substrates, with an efficient barrier against molecular oxygen and moisture. On top of the Barix substrate, a 10 nm (nominal thickness) of aluminium thin film has been deposited by thermo-joule deposition in UHV. The obtained semi-transparent aluminium cathode reduces the transmittance of the bare Barix substrate by 20% in the visible range (from 380 to 700 nm) whereas the electrical resistivity of the Al cathode is 150 Ω cm^{-2}. A 50 nm thick thin film of gold was finally UHV deposited on top of the structure as an anode contact (figure 1). The hole transport layer, namely the α-NPB, has been optimized for maximum current transport and kept constant for the investigated OLEDs devices. Conversely, the Alq3 deposition rate has been varied, with the aim of optimizing electron transport, electron–hole recombination and radiative emission. In fact, in the standard device architecture considered, the Alq3 acts both as an electron transport material and as a light-emitting moiety. We have found that the 65 nm thick Alq3 films grown at a rate of 1 Å s^{-1} or higher show a compact glassy-like morphology and optimal electrical current transport properties.

When the Alq3 deposition rate is decreased to 0.15 Å s^{-1}, the morphology of the obtained film is polycrystalline, still interconnected but with an average grain size of the order of hundreds of nanometres. LSCM images of the deposited films grown at different rates are reported in figure 2.

The physical observable producing the images is the luminescence that is photoemitted from the Alq3 film. The different morphologies of the two films are clearly visible, comparing the LSCM results of figures 2(a) and (b).

We have consequently studied the EL efficiency of OLEDs, keeping constant all the parameters but with different deposition rates for the Alq3 film only. In particular, three different deposition rates have been fixed for the Alq3 film, namely 0.1 Å s^{-1} (‘low’), 1.1 Å s^{-1} (‘high’) and 1.0 $\rightarrow$ 0.3 Å s^{-1} (‘gradient’), where the latter means that the deposition rate has been changed from 1.0 to 0.3 Å s^{-1} during growth of the 65 nm thick Alq3 layer. The three different OLED devices have been moved into the OMBD analysis chamber for EL efficiency comparison. The results are reported in figure 3. Light emission occurs from all three OLEDs devices. The voltage emission onset moves from 9 V (‘low’) to 4 V (‘high’) and 5 V (‘gradient’).

Moreover, the most impressive improvement relates to EL efficiency (note the logarithmic scale) and is shown by the ‘gradient’ OLED devices. This behaviour of the OLEDs seems to

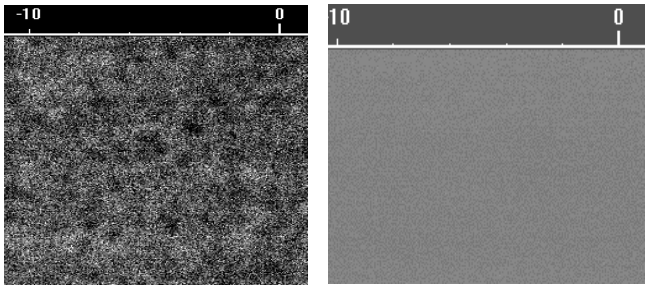

a) b)

Figure 2. Laser scanning confocal microscopy images (10 μm × 10 μm) of 65 nm Alq_3 films grown with different deposition rates: (a) 0.15 Å s^{-1}, (b) 2.1 Å s^{-1}; the Alq3 film has been grown on a Barix/Al substrate. The excitation wavelength was 400 nm, obtained with the second harmonic of a Ti–sapphire laser.

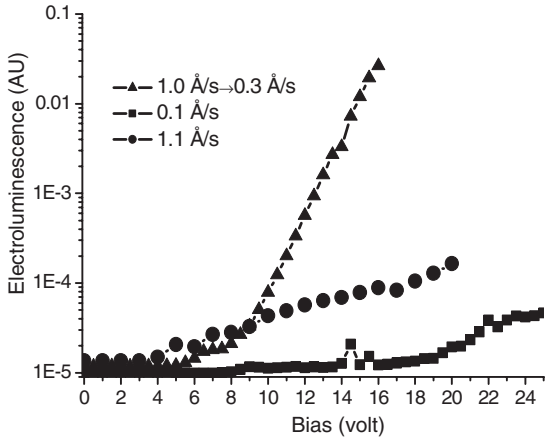

Figure 3. *V*–*L* characteristics of OLEDs with different Alq_3 deposition rates. The different symbols relate to given deposition rates of the Alq3 moiety, whereas the α-NPB has been kept constant for all the devices. These OLEDs were built on a Barix/Al flexible substrate. Among the UHV measured samples, the device made by changing the Alq3 deposition rate from 1.0 → 0.3 Å s^{-1} (triangle) shows the highest light-emitting efficiency.

validate our expectations: the change in the deposition rate leads to differences in the grain size in the Alq_3 layer, optimizing the radiative relaxation of the OLED device. In fact, the obtained experimental results may be interpreted with the following arguments: (i) small grain sizes at the interface with the cathode assure a good electron injection process; (ii) on the other side, at the interface with the hole injection layer, bigger grain sizes are desirable in order to reduce the number of grain boundaries. At the grain boundaries, in fact, the probability of a non-emitting decay of excitons (that can migrate for dozens of nanometres and then dissociate at the grain boundaries) increases. This picture is modelled in figure 4, where an image summarizes our analysis.

3.2. Thermal stabilization of OLED morphology of the films

One typical current behaviour of a standard glass ITO/α-NPB/Alq_3/Al OLED is reported in figure 5. The OLED device has been operated continuously in UHV over the reported time

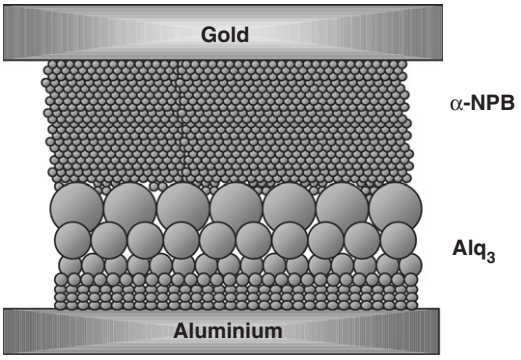

Figure 4. A model of grain sizes distribution in the Alq_3 that could explain the L–V curves obtained with a variable deposition rate. The differences in grain sizes are due to the different deposition rates of organic thin films. These differences are particularly important in the Alq_3, where two critical processes occur: the injection of electrons (much lower mobility than holes) and excitons decay. Small grain dimensions at organic/metal interfaces facilitate charges injections and charge transport leading to higher charge balance in the device. At the interface of Alq_3 with the holes transport layer, larger particles give rise to a small amount of grain boundaries, sites of non-radiative decay of excitons.

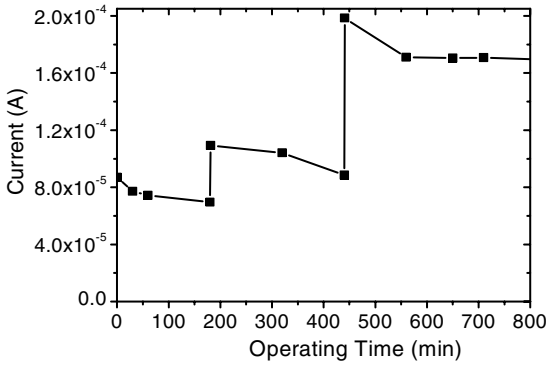

Figure 5. The current behaviour of an OLED measured after its preparation. The OLED device has been operated continuously in UHV over the reported time period, at a constant voltage of 7.5 V. The dc current has been derived from I–V curves and measured at 10 V. The curve is characterized by big fluctuations, probably due to a readjustment in the film's morphology.

period, at a constant voltage of 7.5 V. The dc current has been derived from I–V curves and measured at 10 V. Large fluctuations of the OLED current over time are clearly visible and this reproducible behaviour is characteristic of a standard vacuum-grown OLED at room temperature. Changes of the charge transport through the device could be induced by changes in the morphology of the films after the fabrication of the device. Organic solid materials are polymorph and most probably, after the deposition, organic films are not in their lowest energetic configuration and, until they do not reach this arrangement, the devices will be unstable. In particular, this instability may affect the charge transport, inducing time-sensitive fluctuations in the measured current. In order to induce stability in the OLEDs current behaviour, we tried to supply energy (through a thermal annealing treatment) to induce stable structural conformation in the OLED device. Similarly to what has been reported already in the literature [14–17], we started a systematic study of thermal annealing at different temperatures

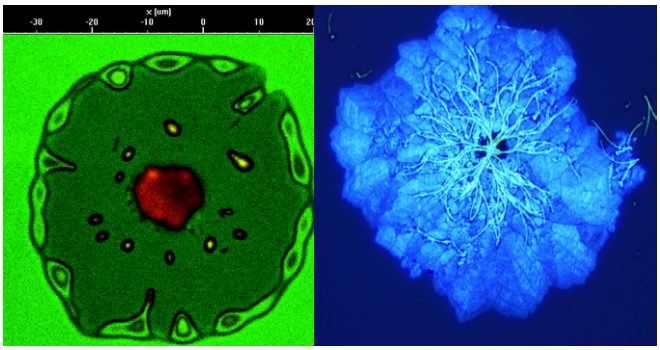

Figure 6. The re-crystallization in organic thin film induced by an annealing temperature higher than the α-NPB glass transition temperature. The annealing temperature was 130 °C, whereas the Alq3 and the α-NPB glass transition temperatures are 177 and 95 °C, respectively. The dramatic effects induced in the organic semiconducting materials are clearly visible. The mass transport occurring between the anode and the cathode of the OLED compromises the device operation.

and time conditions, but with the aim of optimizing the EL properties together with high operation stability over a long operating time of the OLED device. For this purpose, the investigated OLEDs have been grown, thermally processed and measured in UHV. In this way, we can reduce or avoid the degradation and the contamination induced by molecular oxygen and moisture occurring for standard OLEDs operated and characterized in a normal atmosphere. In other words, we have designed the experiment with the maximum attention to avoid the concomitant spurious effects (such as environment-induced degradation of the electrical properties) on the targeted thermal annealing processing for improved current stability. The investigated standard OLED is formed by two different molecular systems, namely the Alq3 and the α-NPB. The deposition rates and film thickness have been kept fixed, as discussed above in section 3.1. The α-NPB moiety possesses a glass transition temperature (t_g) of 95 °C [18], whereas the Alq3 moiety is of 177 °C [19]. We decided to process the standard OLED at 130 °C for 1 h in the OMBD apparatus and then leave the system to recover to room temperature. The *in situ* measured I–V characteristic of this 130 °C annealed OLED shows ohmic behaviour typical of a short-circuited device. The reason for this appears clear from LSCM investigation. In figure 6, the LSCM imaging of the OLED device removed from the OMBD system is reported. The effect of the 130 °C annealing on the morphology of the organic layers is dramatic. The OLED shows a large and evident effect of re-crystallization of the organic component, with mass redistribution and consequent damage of the OLED device.

We then decided to change the annealing temperature to 85 °C. The usual standard OLED has been processed in UHV at 85 °C for 3 h. This time the OLED I–V curve shows the typical diode behaviour and there is electro-emission of light from the Alq3 emitter. Nevertheless, as we can see in figure 7, the OLED current is not stable at all and still shows fluctuations. Following our hypothesis, it means that there are still morphological-structural changes occurring in the organic semiconducting layers. Without removing the OLED from the UHV further, we annealed the same device for 30 h at 85 °C. In this case (see figure 7), as the annealing time is lengthened one order of magnitude, the current become stable. Its value measured at 10 V remains 0.38 ± 0.02 mA for more than 20 h of working time of the measured OLED, continuously operated at 7.5 V over one month. The obtained result can be interpreted in terms of a stable structural configuration induced in the investigated OLED device by the given condition of thermal annealing. A complete *in situ* electro-optical characterization is

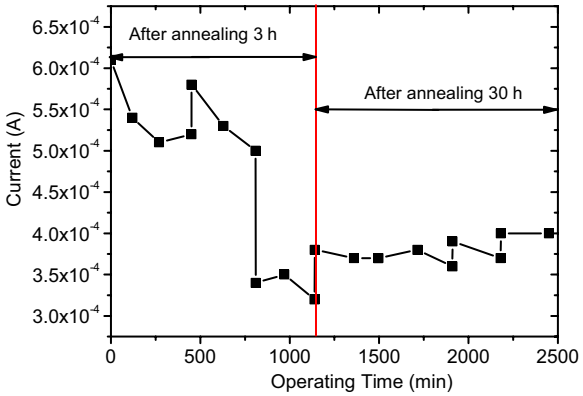

Figure 7. Graph of the OLED current behaviour versus operating time in UHV. The OLED was operated at 7.5 V for about 2500 min. Values of current at 10 V were extrapolated from I–V data collected corresponding to points labelled in the graph. After an annealing time of 3 h at 85 °C, current fluctuations do not disappear (left side). The lengthening of the annealing time at 85 °C to 30 h (right side) makes the OLED current trend stable at 0.38 ± 0.02 mA.

planned for comparison of the EL efficiency gain and the properties of thermally processed OLEDs.

4. Conclusion

We have designed and demonstrated a method to enhance the light emission efficiency in a standard organic light emitting diode by changing the growth parameters, namely the deposition rate, during Alq_3 deposition. We have demonstrated the possibility of obtaining different dimensions of grains in the organics layers during the deposition process. These changes could optimize both the charge injection and radiative decay of excitons, leading to an enhancement of device efficiency.

At the same time, with the objective of controlling and stabilizing the morphology changes and stabilizing the charge transport over a long operating time, we have studied the effect of thermal annealing processing in the standard current behaviour of OLEDs. By optimizing the annealing temperature and the annealing time, we have assessed the stabilization of the current flux through standard OLED devices. The supplied thermal energy has been able to induce stabilization of the film structure, leading the morphology to the lowest energetic configuration. The stabilization of the structure of the films removes the cause of the current fluctuations observed in non-treated devices.

Acknowledgments

This work was carried out within the European Union's EUREKA project E!2541 FOLIA (Flexible Organic Illuminators for the Automotive market) and funded by the Italian MIUR (Ministero dell' Istruzione, dell' Università e della Ricerca).

References

[1] Shen Z, Burrows P E, Bulović V, Forrest S R and Thompson M E 1997 *Science* **276** 2009
[2] Brutting W, Berleb S and Muckl A G 2001 *Org. Electron.* **2** 1

[3] *OIDA Report* August 2002
Melpignano P, Biondo V, Sinesi S, Gale M T, Westenhöfer S, Murgia M, Caria S and Zamboni R 2006 *Appl. Phys. Lett.* **88** 153514
[4] Nakanotani H, Oymada T, Kawamura Y, Sasabe H and Adachi C 2005 *Japan. J. Appl. Phys.* **44** 3659
[5] Melpignano P, Baron-Toaldo A, Biondo V, Priante S, Zamboni R, Murgia M, Caria S, Gregoratti L, Barinov A and Kiskinova M 2005 *Appl. Phys. Lett.* **86** 041105
[6] Mandai M, Takarda K, Aoki T, Fujinarni T, Nakanishi Y and Hataneks Y 1997 *Synth. Met.* **91** 12
[7] Chen B J, Lai W Y, Gao Z Q, Lee C S, Lee S T and Gambling W A 1999 *Appl. Phys. Lett.* **75** 4010
[8] Garbuzov D Z, Bulović V, Burrows P E and Forrest S R 1996 *Chem. Phys. Lett.* **249** 433
[9] Burrows P E and Forrest S R 1994 *Appl. Phys. Lett.* **64** 2285
[10] Chen L F, Liao L S, Lai W Y, Sun X H, Wong N B, Lee C S and Lee S T 2000 *Chem. Phys. Lett.* **319** 418
[11] Lee C B, Uddin A, Hu X and Andersson T G 2004 *Mater. Sci. Eng.* B **112** 14
[12] Forrest S R 1997 *Chem. Rev.* **97** 1793
[13] Loi M A, Da Como E, Zamboni R and Muccini M 2003 *Synth. Met.* **139** 687
[14] Lee T and Park O O 2000 *Adv. Mater.* **12** 801
[15] Kirn J, Lee J, Han C W, Lee N Y and Chung I J 2003 *Appl. Phys. Lett.* **82** 4238
[16] Sun M C, Jou J H, Weng W K and Huang Y S 2005 *Thin Solid Films* **491** 260
[17] Chen B J, Sun X W, Wong T K S, Hu X and Uddin A 2005 *Appl. Phys. Lett.* **87** 063505
[18] Van Slyke S A, Chen C H and Tang C W 1996 *Appl. Phys. Lett.* **69** 2160
[19] Shen J Y, Lee C Y, Huang T H, Lin J T, Tao Y, Chien C and Tsai C 2005 *J. Mater. Chem.* **15** 2455